Multi-component structure of nonlinear excitations in systems with length-scale competition

P.L. Christiansen[1], Y.B. Gaididei[2], F.G. Mertens[3], and S.F. Mingaleev[2,a]

[1] Department of Mathematical Modelling, The Technical University of Denmark, 2800 Lyngby, Denmark
[2] Bogolyubov Institute for Theoretical Physics, 03143 Kiev, Ukraine
[3] Physikalisches Institut, Universität Bayreuth, 95440 Bayreuth, Germany

Abstract. We investigate the properties of nonlinear excitations in different types of soliton carrying systems with *long-range dispersive interactions*. We show that length-scale competition in such systems, universally results in a multi-component structure of nonlinear excitations which may lead to a *new type of multistability*: coexistence of different nonlinear excitations at the same value of the *spectral parameter* (*i.e.*, velocity in the case of anharmonic lattices or frequency in nonlinear Schrödinger models).

PACS. 05.45.Yv Solitons – 02.70.Hm Spectral methods – 42.65.Pc Optical bistability, multistability, and switching

1 Introduction

Physical systems with competition between discreteness, nonlinearity and dispersion are abundant in nature. Examples are nonlinear charge and energy transport in biological macromolecules, elastic energy transfer in anharmonic chains, charge transport in hydrogen-bonded systems, coupled optical fibers, nonlinear photonic crystals, arrays of coupled Josephson junctions. Determination of their dynamical properties is of importance because of their wide applicability in various physical problems. In nonlinear systems with short-range (nearest-neighbor) dispersive interactions there are basically two types of nonlinear excitation. In the large dispersion (weak nonlinearity) limit when the discreteness of the lattice plays no essential role, the balance between nonlinearity and dispersion provides the existence of low-energy soliton-like excitations. The width of these excitations is large compared with the lattice spacing. They freely propagate along the system without energy loss, and their collisions are almost elastic. When the nonlinearity is strong (dispersion is weak) new nonlinear excitations, intrinsically localized modes, also called discrete breathers, may appear (see *e.g.* Ref. [1] for a review). Their width is comparable with the lattice spacing, and they are long-lived and robust.

The phenomenon of multistability, implying the coexistence of several stationary localized states having the same energy, appears in different contexts [2–14]. For the one-dimensional discrete nonlinear Schrödinger (NLS) equation with nearest-neighbor interactions (NNI) and ar-

bitrary power of nonlinearity, multistability occurs when the power exceeds some critical value [2–4].

Another mechanism of such multistability comes out for the systems with long-range dispersive interactions, where a new characteristic length scale appears: the radius of the dispersive interaction. As it was shown in references [5–10] the appearance of the new characteristic length scale brings into coexistence two stable stationary excitations; a broad, continuum-like soliton and a narrow discrete excitation. This is a generic property of nonlinear systems with nonlocal dispersive interactions. The bistability occurs in such different systems as anharmonic chains with nonlocal interatomic interaction [5–7], NLS models with long-range coupling [8,9], and nonlinear waveguides in photonic crystals [10]. In all these systems the bistability means that there is an interval of the energy H where two stable nonlinear excitations (one of which is broad and another is intrinsically localized) coexist for each value of H. The greater the radius of the long-range interactions, the more pronounced is the bistability phenomenon. A general mechanism for obtaining a controlled switching between bistable localized excitations was proposed in references [11,12]. Importantly, very similar types of excitations may appear in periodic nonlinear dielectric superlattices (two-dimensional nonlinear Kronig-Penney model [13]) where the nonlocality arises as a result of a reduction of the original two-dimensional problem to an effective one-dimensional description. Bistability in the spectrum of nonlinear localized excitations in magnets with a weak exchange interaction and strong magnetic anisotropy was found in reference [14].

[a] e-mail: `smino@bitp.kiev.ua`

Quite recently coexistence of different nonlinear excitations at *the same value of the soliton velocity* has been shown to take place in anharmonic chains with *ultra-long-range* interatomic interactions [15]. Specifically, it was shown that three different types of pulse solitons can coexist for each value of the pulse velocity in a certain velocity interval: one type is unstable but the two others can be stable. It should be emphasized the following intriguing aspect of the problem: in contrast to the previously discussed cases, now the bistability takes place at the same value of a *spectral parameter* (the soliton velocity in this system is mathematically the spectral parameter of a nonlinear eigenvalue problem). Therefore, the system being discussed provides us with the example of a *new type of multistability* whose physical consequences can be quite different from the multistability discussed above.

The aim of the present paper is to demonstrate that the new type of multistability is a fundamental property of nonlinear systems with ultra-long-range dispersion. To this end we consider two additional (in comparison with Ref. [15]) models: a discrete NLS equation with nonlocal dispersion and an anharmonic lattice with screened Coulomb interaction. We show that in both cases an *ultra-long-range* dispersive interaction results in a *multi-valued dependence* of the energy of stationary states on a spectral parameter (frequency in the case of the NLS equation and velocity in the case of the anharmonic lattice).

The outline of the paper as follows. In Section 2 we present the results of numerical simulations of stationary states in the discrete NLS model with a long-range dispersive interaction and in the anharmonic chain with a long-range dispersive interaction and cubic nearest-neighbor interaction. We discuss the appearance of a multi-valued dependence of the energy of the systems. In Section 3 we develop an analytical approach to the problem. We use a quasicontinuum approach which preserves both length scales that enter our problem. We show that the low-energy excitation can be considered as a compound state: a short-range breather-like component and a long-ranged component. Section 4 presents the concluding discussion.

2 Models and numerical results

We consider in parallel two nonlinear models which can bear pulse-like excitations: the Boussinesq equation model which describes the properties of anharmonic molecular chains and the nonlinear Schrödinger equation model which represents generic properties of a system of nonlinear oscillators.

2.1 Anharmonic chains with ultra-long-range dispersive interactions

Let us consider a chain of equally spaced particles of unit mass with displacements from equilibrium $u_n(t)$ and with an equilibrium spacings at unity. The Hamiltonian of the system is given by

$$H = \sum_n \left\{ \frac{1}{2}\left(\frac{du_n}{dt}\right)^2 + V(u_{n+1} - u_n) \right.$$
$$\left. + \frac{1}{2}\sum_{m>n} J_{m-n}(u_m - u_n)^2 \right\}, \qquad (1)$$

with the anharmonic interaction

$$V(w) = w^2/2 - w^3/3 \qquad (2)$$

between nearest neighbors and the harmonic long-range interaction (LRI)

$$J_{m-n}(\alpha, s) = J(\alpha, s)\frac{e^{-\alpha|m-n|}}{|m-n|^s} \qquad (3)$$

between all particles of the chain. Here

$$J(\alpha, s) = J/F(e^{-\alpha}, s), \qquad (4)$$

where

$$F(z, s) = \sum_{n=1}^{\infty}(z^n/n^s) \qquad (5)$$

is the so-called Joncqière's function which properties are described in reference [16]. J characterizes the intensity of the LRI's whereas α and s determine their inverse radius. The coefficient $J(\alpha, s)$ is chosen in the form (4) to have the sum $\sum_n J_n(\alpha, s)$ independent of α and s. The parameters α and s are introduced to cover different physical situations from the limit of nearest-neighbor interactions ($\alpha \gg 1$ or $s \gg 1$) to the limit of ultra-long-range interactions ($\alpha \ll 1$ and $s \leq 3$). The Hamiltonian (1) generates equations of motion of the form

$$\frac{d^2 w_n}{dt^2} + 2W(w_n) - W(w_{n+1}) - W(w_{n-1})$$
$$+ \sum_{m \neq n} J_{m,n}(w_n - w_m) = 0, \qquad (6)$$

where $w_n = u_{n+1} - u_n$ are relative displacements and $W(w) \equiv dV(w)/dw = w - w^2$. We use the quasicontinuum approach, regarding n as a continuous variable: $n \to x$, $w_n(t) \to w(x, t)$, and using the operator identities

$$w(x + m, t) = e^{m\partial_x}w(x, t),$$
$$Q(\alpha, s, \partial_x) \equiv \sum_{m=1}^{\infty} \frac{e^{-\alpha m}}{m^s}\frac{1 - \cosh m\partial_x}{F(e^{-\alpha}, s)}$$
$$= 1 - \frac{F(e^{-\alpha-\partial_x}, s) + F(e^{-\alpha+\partial_x}, s)}{2F(e^{-\alpha}, s)}. \quad (7)$$

In this approach the equation of motion (6) can be written in the pseudo-differential form

$$[\partial_t^2 - JQ(\alpha, s, \partial_x)]w(x, t) - 4\sinh^2\left(\frac{\partial_x}{2}\right)W(w) = 0,$$
$$(8)$$

where ∂_x and ∂_t are the derivatives with respect to x and t, respectively. Equation (8) can be called *non-local Boussinesq equation*.

The energy (1) together with the momentum

$$P = \int_{-\infty}^{\infty} \left(\frac{\partial u}{\partial t}\right)\left(\frac{\partial u}{\partial x}\right) \mathrm{d}x \qquad (9)$$

are conserved quantities. We are interested in the stationary soliton solutions $w(x,t) \equiv w(x - vt)$ propagating with velocity v. Substituting $z = x - vt$ we can write equation (8) in the form

$$[v^2\partial_z^2 - JQ(\alpha, s, \partial_z)]w(z) - 4\sinh^2\left(\frac{\partial_z}{2}\right)W(w) = 0 . \qquad (10)$$

In this way we reduce our problem to a nonlinear eigenvalue problem with v being a spectral parameter.

We consider two physically important cases: screened Coulomb interactions ($s = 3$) and the Kac-Baker LRI's ($s = 0$). The speed of sound c (which is an upper limit of the group velocity of linear waves), determined by the expression $c^2 = 1 + JF\left(\mathrm{e}^{-\alpha}, s - 2\right)/F\left(\mathrm{e}^{-\alpha}, s\right)$, grows indefinitely in both cases as α decreases. Using the Green's function method [7] one can show that spatially localized stationary solutions (solitons) exist only for supersonic velocities $v > c$.

We have numerically integrated equation (10) using the method developed in reference [7]. Figures 1 and 2 show the dependence of the energy $H(v)$ (the dependence $P(v)$ has the same form) of the soliton solutions of equation (10) obtained for the Kac-Baker interaction ($s = 0$) and screened Coulomb interaction ($s = 3$), respectively. It is seen that the behavior in both cases is qualitatively the same. The soliton energy grows *monotonically* with the velocity in the case of large α (see, *e.g.*, $\alpha = 0.3$ in Fig. 1). In this case the soliton properties are qualitatively the same as in the limit of nearest-neighbor interactions (NNI's) for which equation (8) reduces to the Boussinesq equation. It is well known that this equation has a sech-shaped soliton solution $w(z) = -1.5\,(v^2 - c^2)/\cosh^2(\sigma z)$, where $\sigma = \sqrt{3(v^2 - c^2)}$ is the inverse soliton width. As indicated above, the energy $H \sim (v^2 - c^2)^{3/2}$ of these solitons is a monotonic function of the velocity, which means that there is only one soliton solution for each given value of energy or velocity.

The situation changes when $\alpha < \alpha_{cr}$ (*e.g.*, for the Kac-Baker interaction the critical value of inverse radius $\alpha_{\mathrm{cr}}(J)$ is determined by Eq. (9) in Ref. [15]). In this case, as was shown first in reference [6], the dependence $H(v)$ becomes *non-monotonic* (of N-shape, with a local maximum and a local minimum), so that there exist two branches of *stable* supersonic solitons: low-velocity and high-velocity solitons. These two soliton branches are separated by a *gap* (an interval of velocities where $H(v)$ decreases) with *unstable* soliton states. It is interesting that because of the non-monotonic dependence of $H(v)$ there exist low-velocity and high-velocity solitons of equal energy. Further increasing of the radius of the dispersive interaction (decreasing α) leads to a Z-shape dependence of $H(v)$ (see
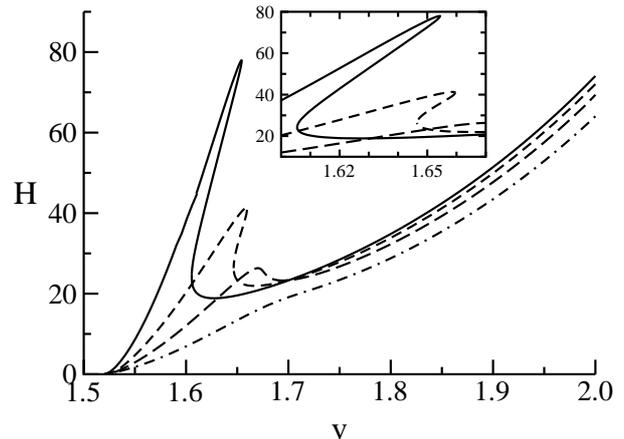

Fig. 1. Energy of the pulse solitons *versus* velocity in the anharmonic lattice with Kac-Baker ($s = 0$) long-range interaction found numerically for different values of α and J (the value of J was chosen to get constant $c = 1.515$): $\alpha = 0.05$ and $J = 0.0016$ (full line); $\alpha = 0.1$ and $J = 0.0062$ (dashed line); $\alpha = 0.17$ and $J = 0.0172$ (long-dashed line); $\alpha = 0.3$ and $J = 0.05$ (dot-dashed line).
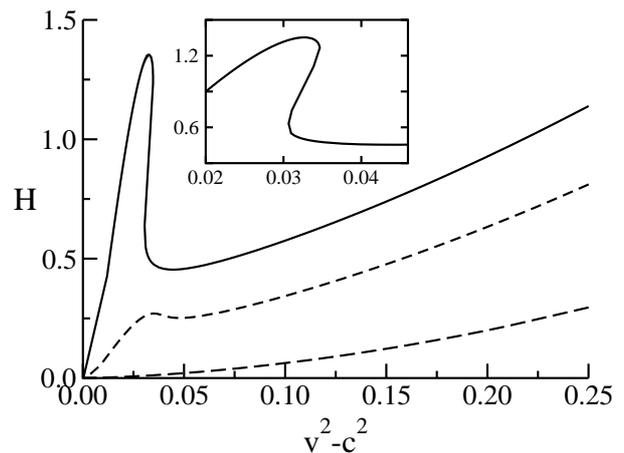

Fig. 2. Energy of the pulse solitons *versus* velocity in the anharmonic lattice with screened Coulomb ($s = 3$) interaction for $J = 0.05$ and different values of α: $\alpha = 0.001$ (full line), $\alpha = 0.005$ (dashed line), and $\alpha = \infty$ (long-dashed line).

Figs. 1 and 2). In this case the gap which separated two above-mentioned soliton branches collapses; instead, there appears an interval of velocities where three soliton solutions with different energies and shapes (see Figs. 3 and 4) coexist for each value of velocity. This phenomenon was first observed in reference [15] for the Kac-Baker dispersive interaction. Here we show that the same phenomenon takes place also in the case of the screened Coulomb interaction, but the radius of the interaction should be much larger: *e.g.*, for the Coulomb dispersive interaction with the intensity $J = 0.05$ the gap vanishes for $\alpha < 0.0015$ while for the Kac-Baker interaction with the same intensity J it happens for $\alpha < 0.15$.
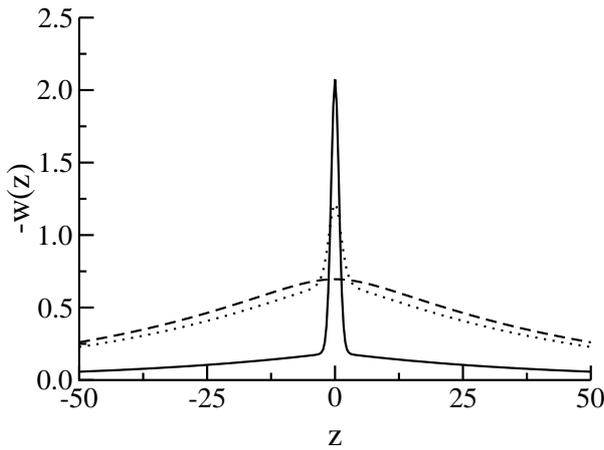
Fig. 3. Shapes of the low-energy (full line), unstable intermediate-energy (dotted line), and high-energy (dashed line) pulse solitons which coexist at the same velocity $v = 1.64$ in the anharmonic lattice with Kac-Baker ($s = 0$) long-range interaction for $\alpha = 0.05$ and $J = 0.0016$ (see Fig. 1).

Fig. 4. Shapes of the low-energy (full line) and high-energy (dashed line) pulse solitons which coexist at the same velocity $v^2 - c^2 = 0.031$ in the anharmonic lattice with screened Coulomb ($s = 3$) interaction for $J = 0.05$ and $\alpha = 0.001$ (see Fig. 2).

2.2 The nonlinear Schrödinger model with ultra-long-range dispersive interaction

Let us now consider a system of coupled nonlinear oscillators which is described by the Hamiltonian

$$H = \frac{1}{2} \sum_n \left\{ \sum_{m \neq n} J_{n-m}(\alpha, s) |\psi_n - \psi_m|^2 - |\psi_n|^4 \right\} , (11)$$

where n and m are site indices, and ψ_n is the excitation wave function. The first term in equation (11) describes a dispersive interaction between nonlinear oscillators. The second one represents a nonlinear interaction in the system. The case $\alpha = 0$ in the dispersive interaction has been studied in detail in reference [9]. Here we consider the dispersive interaction $J_{n-m}(\alpha, s)$ in the Kac-Baker form ($s = 0$):

$$J_{n-m} = J(e^\alpha - 1) e^{-\alpha|n-m|} . \tag{12}$$

It is important to investigate this type of the dispersive interaction because real physical systems which are described by the Hamiltonian (11) with the dispersive interaction given by equation (12) are not rare. For example, such type of excitation transfer may take place in systems where the dispersion curves of two elementary excitations are close or intersect and effective long-range transfer occurs at the cost of the coupling between excitations. This is the case for excitons and photons in semiconductors and molecular crystals. Dynamics of nonlinear photonic band-gap materials and periodic nonlinear dielectric superlattices is described [13] by equations which are closely related to the equations which govern the dynamics of the discrete NLS model with the dispersive interaction in the Kac-Baker form (12). It was shown in reference [13] that the radius of the effective dispersive interaction is proportional to the distance between nonlinear layers. Therefore
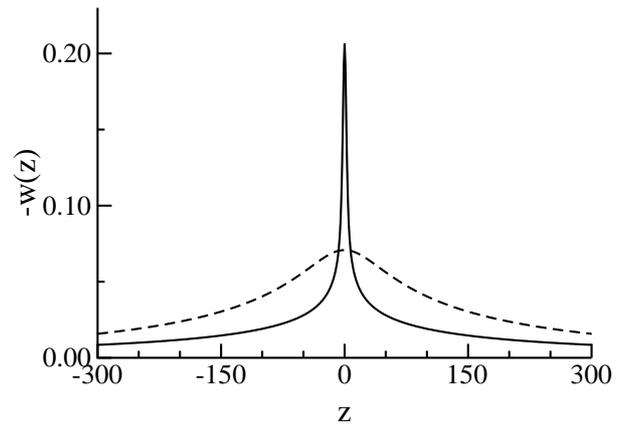
one can easily tune the range of the dispersive interaction by preparing nonlinear lattices with different spacing between nonlinear layers.

In the Hamiltonian (11) ψ_n and $i\psi_n^*$ are canonically conjugated variables and the equation of motion $i\frac{d}{dt}\psi_n = \partial H/\partial \psi_n^*$ has the form

$$i\frac{d\psi_n}{dt} + \sum_m J_{n-m} (\psi_m - \psi_n) + |\psi_n|^2 \psi_n = 0 . \tag{13}$$

The energy of the system H together with the number of quanta

$$N = \sum_n |\psi_n|^2 \tag{14}$$

are conserved quantities.

We study stationary states of the system

$$\psi_n(t) = \phi_n(\Lambda) e^{i\Lambda t} , \tag{15}$$

where Λ is the nonlinear frequency and $\phi_n(\Lambda)$ is the amplitude at the n-th site. For small and intermediate radius (α^{-1}) of the dispersive interaction the problem was studied in references [11]. It was shown that for $\alpha < 1.7$ the NLS model exhibits bistability in the spectrum of nonlinear stationary states: for each value of N in the interval $[N_l(\alpha), N_u(\alpha)]$ there exist three stationary states with frequencies $\Lambda_1(N) < \Lambda_2(N) < \Lambda_3(N)$. Since for discrete NLS equations a necessary and sufficient condition for linear stability of stationary states with a single maximum at a lattice site is $dN/d\Lambda > 0$ (see, *e.g.*, Ref. [2]), the low-frequency $\Lambda_1(N)$ and high-frequency $\Lambda_3(N)$ states, for which $dN/d\Lambda > 0$, are stable (in what follows we shall refer to them as to the 'low-frequency branch' and 'high-frequency branch'). There is an interval ('gap') of the nonlinear frequency Λ which separates two branches of nonlinear excitations. Figures 5 and 6 show H *versus* Λ and N *versus* Λ, respectively, obtained from direct numerical solution of equation (13) for different values of the

Fig. 5. Energy H of the stationary solitons versus nonlinear frequency Λ in the NLS model with Kac-Baker ($s = 0$) long-range interaction for different values of α: 0.1 (full line), 0.3 (dashed line), 0.7 (long-dashed line), and ∞ (dot-dashed line).
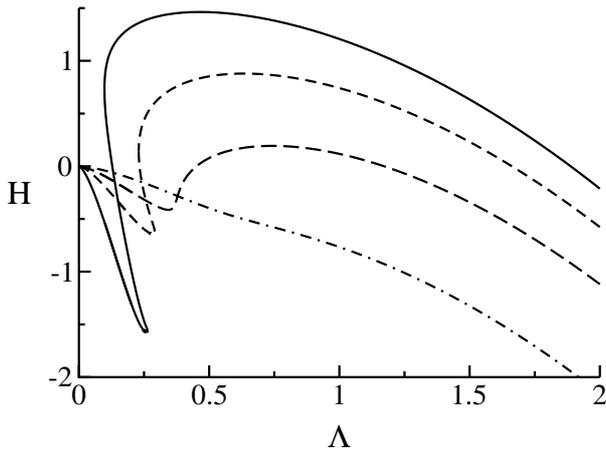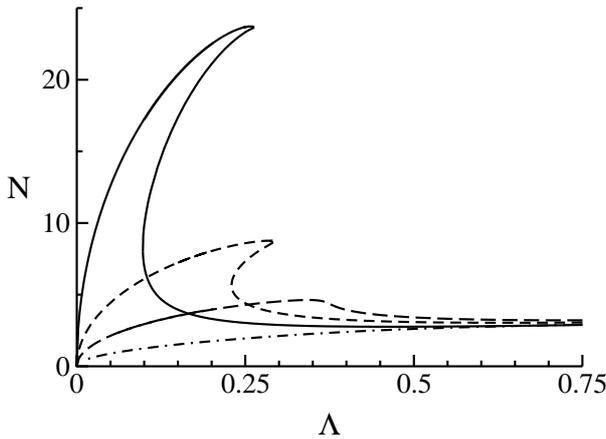

Fig. 6. Number of quanta N of the stationary solitons *versus* nonlinear frequency Λ in the NLS model with Kac-Baker ($s = 0$) long-range interaction for different values of α: 0.1 (full line), 0.3 (dashed line), 0.7 (long-dashed line), and ∞ (dot-dashed line).

inverse radius of dispersive interaction α. It is seen that similar to the case of the nonlocal Boussinesq equation the gap decreases when the radius of the dispersive interaction increases until eventually it vanishes.

Comparing Figures 1 and 2 obtained for the Boussinesq model with Figure 5 obtained for the NLS model we see that several new but common features arise as a consequence of the ultra-long-range dispersive interaction:

- The gap which separates the two branches of stable stationary solutions decreases when the radius of the dispersive interaction α^{-1} increases.
- For small enough α (in the NLS model for $\alpha < 0.57$) three different stationary states coexist for each value of spectral parameter (velocity v in the case of the Boussinesq equation and nonlinear frequency Λ in the NLS model). These three states are characterized by different values of the integrals of motion: the energy
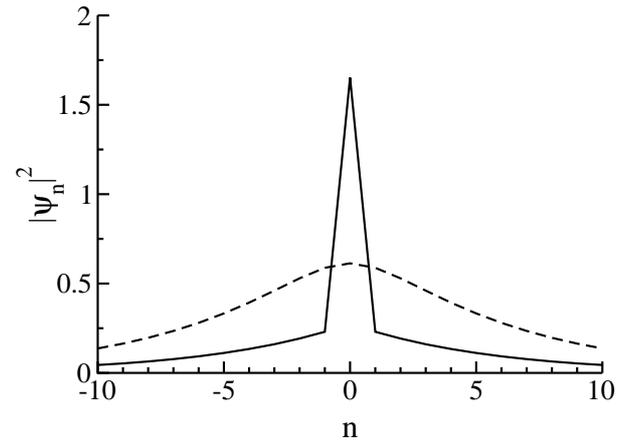

Fig. 7. Shapes of the high-energy (full line) and low-energy (dashed line) stationary solitons which coexist at the same non-linear frequency $\Lambda = 0.25$ in the NLS model with Kac-Baker long-range interaction for $\alpha = 0.3$ (see Fig. 5).

H (in both models) and either the number of quanta N (for the NLS equation) or the momentum P (for the Boussinesq equation).
- The shapes of these states differ significantly (see Figs. 3–4 and 7). The high-energy state is broad and continuum-like while the low-energy states consist of two components, short-range and long-range ones. The width of the short-range component is of a few lattice spacing while the long-range component has tails which spread out a few tens of lattice constants.
- The state with an intermediate energy is always unstable while the stability of two other states depends on the radius of the dispersive interaction α^{-1}. For example, in the case of the NLS equation for $\alpha > 0.03$ the state which belongs to the high-frequency branch is unstable ($\mathrm{d}N/\mathrm{d}\Lambda < 0$ for these α). But this state becomes stable when $\alpha < 0.03$.

3 Analytical approach

In our analytical approach we will be mostly concerned with the case of the NLS equation model because an analytical theory of multi-component solutions of the nonlocal Boussinesq equation is partially presented in references [6,7].

3.1 Nonlinear Schrödinger equation model

In the quasicontinuum approach, regarding n as a continuous variable: $n \to x$, $\psi_n(t) \to \psi(x,t)$, equation (13) can be written as

$$\mathrm{i}\partial_t\psi + \frac{J}{2}\,Q(\alpha, s = 0, \partial_x)\psi + |\psi|^2\psi = 0 \,, \qquad (16)$$

where

$$Q(\alpha, s = 0, \partial_x) = (\mathrm{e}^\alpha + 1)\frac{4\sinh^2(\partial_x/2)}{\kappa^2 - 4\sinh^2(\partial_x/2)} \qquad (17)$$

with $\kappa = 2\sinh(\alpha/2)$ being a range parameter, is a linear pseudo-differential operator for the Kac-Baker dispersive interaction (12).

In order to obtain an analytic solution of the pseudo-differential equation (16) we use an approach akin to the previously proposed in reference [17]: we multiply equation (16) by the operator $\frac{\partial_x^2}{4\sinh^2(\frac{\partial_x}{2})}$ and expand in a Taylor series this operator ($\frac{\partial_x^2}{4\sinh^2(\frac{\partial_x}{2})} \approx 1 - \frac{1}{12}\partial_x^2$) as well as the operator $\sinh^2(\partial_x/2)$ in the denominator of the r.h.s. of equation (17). We stress that our modification of the standard continuum approximation is crucial in the preserving the second length scale that enters our problem. As a result we get a pseudo-differential equation

$$\mathrm{i}\left(1 - \frac{\partial_x^2}{12}\right)\partial_t \psi + \frac{J}{2}(\mathrm{e}^\alpha + 1)\frac{\partial_x^2}{\kappa^2 - \partial_x^2}\psi + |\psi|^2\psi = 0 , \quad (18)$$

where the small term $\frac{1}{12}\partial_x^2|\psi|^2\psi$ was omitted.

Looking for stationary solutions

$$\psi = \sqrt{\frac{J}{2}(\mathrm{e}^\alpha + 1)}\,\Phi(x)\,\mathrm{e}^{\mathrm{i}\Lambda\tau} , \quad (19)$$

where $\tau = \frac{J}{2}(\mathrm{e}^\alpha + 1)t$, we can write equation (18) in the form

$$(\partial_x^2 - s_+^2)(\partial_x^2 - s_-^2)\Phi + \frac{12}{\Lambda}(\partial_x^2 - \kappa^2)\Phi^3 = 0 , \quad (20)$$

with the parameters $s_\pm$ given by

$$s_\pm^2 = \frac{1}{2}\left\{\kappa^2 + 12\frac{\Lambda + 1}{\Lambda}\right.$$
$$\left. \pm \sqrt{\left(\kappa^2 + 12\frac{\Lambda + 1}{\Lambda}\right)^2 - 48\kappa^2}\right\} . \quad (21)$$

In the limit of small α

$$s_-^2 \approx \frac{\Lambda\kappa^2}{\Lambda + 1} , \qquad s_+^2 \approx 12\frac{\Lambda + 1}{\Lambda} . \quad (22)$$

For small nonlinear frequency Λ we expect excitations with a width much larger than s_+^{-1} so that only one scale s_-^{-1} should be important. Since the characteristic width of the excitations of interest here is large as compared with s_+^{-1}, we can neglect the operator ∂_x^2 in the operator $(\partial_x^2 - s_+^2)$ and get

$$(\partial_x^2 - s_-^2)\Phi - \frac{1}{\Lambda + 1}(\partial_x^2 - \kappa^2)\Phi^3 = 0 . \quad (23)$$

This equation was investigated in reference [8]. It was shown that equation (23) has a soliton solution when the inequality $A = (\kappa^2/s_-^2) \geq 9$ holds. As it is seen from equation (22) in the case of small α this inequality reduces to $\Lambda < 1/8$. The number of quanta which corresponds to

the solution of equation (23) has the form

$$N \equiv N_< = s_+^2\Lambda\frac{\kappa}{2\sqrt{A}}\left\{1 + \frac{A - 9}{24}\right.$$
$$\left. \times \ln\left(\frac{(\sqrt{A} + 1)(\sqrt{A} + 3)}{(\sqrt{A} - 1)(\sqrt{A} - 3)}\right)\right\} . \quad (24)$$

For large Λ, when both length-scales are important, we will seek a solution of equation (20) as the sum

$$\Phi = \sqrt{\frac{\Lambda}{12}}\left\{\phi_{\mathrm{S}}(x) + \phi_{\mathrm{L}}(x)\right\} , \quad (25)$$

where $\phi_{\mathrm{S}}(x)$ is the short-range component and $\phi_{\mathrm{L}}(x)$ is the long-range one. Here $\phi_{\mathrm{S}}(x)$ will dominate in the center, while $\phi_{\mathrm{L}}(x)$ in the tails.

Inserting equation (25) into equation (20) yields

$$(\partial_x^2 - s_-^2)\left\{(\partial_x^2 - s_+^2)(\phi_{\mathrm{S}} + \phi_{\mathrm{L}}) + (\phi_{\mathrm{S}} + \phi_{\mathrm{L}})^3\right\}$$
$$-(\kappa^2 - s_-^2)(\phi_{\mathrm{S}} + \phi_{\mathrm{L}})^3 = 0 . \quad (26)$$

Assuming that the function $\phi_{\mathrm{S}}(x)$ satisfies the equation

$$(\partial_x^2 - s_+^2)\phi_{\mathrm{S}} + 3\phi_{\mathrm{L}}(0)\phi_{\mathrm{S}}^2 + 3\phi_{\mathrm{L}}^2(x)\phi_{\mathrm{S}} + \phi_{\mathrm{S}}^3 = 0 , \quad (27)$$

we obtain from equation (26) an equation for $\phi_{\mathrm{L}}(x)$ in the form

$$(\partial_x^2 - s_-^2)(-s_+^2\phi_{\mathrm{L}} + \phi_{\mathrm{L}}^3) + (s_-^2 - \kappa^2)\phi_{\mathrm{L}}^3$$
$$= B(\kappa^2 - s_-^2)\delta(x) , \quad (28)$$

where

$$B = \int_{-\infty}^\infty \mathrm{d}x \left\{\phi_{\mathrm{S}}^3(x) + 3\phi_{\mathrm{L}}^2(x)\phi_{\mathrm{S}}(x) + 3\phi_{\mathrm{L}}(x)\phi_{\mathrm{S}}^2(x)\right\}$$
$$= s_+^2 \int_{-\infty}^\infty \mathrm{d}x\,\phi_{\mathrm{S}}(x) . \quad (29)$$

To obtain equation (28) we took into account the big difference in the short-range scale s_+^{-1} and the long-range scale s_-^{-1}. It permitted us to replace the product $\phi_{\mathrm{L}}(z)\phi_{\mathrm{S}}(z)$ by $\phi_{\mathrm{L}}(0)\phi_{\mathrm{S}}(z)$ in equation (27), to neglect the term $\partial_z^2\phi_{\mathrm{L}}$ as compared with $s_+^2\phi_{\mathrm{L}}$ in the l.h.s. of equation (28) and to replace the function $(\kappa^2 - s_-^2)\{\phi_{\mathrm{S}}^3(x) + 3\phi_{\mathrm{L}}^2(x)\phi_{\mathrm{S}}(x) + 3\phi_{\mathrm{L}}(x)\phi_{\mathrm{S}}^2(x)\}$ by the r.h.s. of equation (28). Also, equation (27) was used in equation (29).

We obtain for the short-range component $\phi_{\mathrm{S}}(x)$ the expression

$$\phi_{\mathrm{S}}(x) = \frac{\sqrt{2}s_+(1 - 3a^2)}{\sqrt{1 - a^2}\cosh(\sqrt{1 - 3a^2}s_+x) + \sqrt{2}a} , \quad (30)$$

where $a = \phi_L(0)/s_+$ is the amplitude of the long-range component.

Equation (28) on the half x-axis subject to the vanishing at infinity boundary conditions can be presented as

$$(s_+^2 - 3\phi_{\mathrm{L}}^2)\partial_x\phi_{\mathrm{L}} =$$
$$-\phi_{\mathrm{L}}\sqrt{s_+^4\,s_-^2 - s_+^2\frac{3\,s_-^2 + \kappa^2}{2}\phi_{\mathrm{L}}^2 + \kappa^2\phi_{\mathrm{L}}^4} \quad (31)$$

with the boundary condition at the origin in the form

$$-2\left(s_+^2 - 3\,\phi_{\mathrm{L}}^2(0)\right)\partial_x\phi_{\mathrm{L}}(+0) = (\kappa^2 - s_-^2)\,B\,. \quad (32)$$

Substituting equations (29–31) into equation (32) we obtain that the amplitude a of the long-range component is determined by the equation

$$\kappa = \frac{a\,R(a)\,A\sqrt{6}}{(A-1)\arccos\sqrt{2a^2/(1-a^2)}}\,, \quad (33)$$

where $R(a) = \sqrt{A\,a^4 - (A+3)\,a^2/2 + 1}$.

The number of quanta which corresponds to the solution (25) is determined by the expression

$$N \equiv N_> = (\Lambda+1)\Bigg(\frac{4}{s_+}\sqrt{1-3a^2} + \frac{6}{\kappa\sqrt{A}}\Big\{1 - R(a)$$
$$+ \frac{A-9}{12\sqrt{A}}\ln\left|\frac{4R(a)+4Aa^2-A-3}{4\sqrt{A}-A-3}\right|\Big\}\Bigg)\cdot \quad (34)$$

When $\kappa > \kappa_{\mathrm{b}}$, where $\kappa_{\mathrm{b}} \approx 0.63$ is the maximum value of the function in the r.h.s. of equation (33) for $A = 9\,(\Lambda = 1/8)$, equation (33) has only one solution in the interval $A < 9\,(\Lambda > 1/8)$. Inserting equation (33) into equation (34) and combining equations (24) and (34) we obtain that the number of quanta N as a function of Λ has an N-type shape (see Fig. 6) with a finite gap which separates two branches of stable solitons. When $\kappa \leq \kappa_{\mathrm{b}}$ the gap collapses and equation (33) has two solutions for $A > 9\,(\Lambda < 1/8)$. Taking into account that for $A > 9$ $(\Lambda < 1/8)$ there exists also a low-frequency solution of equation (23), one can conclude that for $\kappa \leq \kappa_{\mathrm{b}}$ there is an interval of Λ where three stationary states correspond to each value of the nonlinear frequency. In this case the curve $N(\Lambda)$ has a Z-type shape (see Fig. 6). It is worth noticing that the bifurcation value for the inverse radius of the dispersive interaction $\alpha_{\mathrm{b}} \approx 0.61$ $(2\sinh(\alpha_{\mathrm{b}}/2) = \kappa_{\mathrm{b}})$ obtained analytically is in a surprisingly good agreement with the value obtained from numerical simulations $(\alpha_{\mathrm{b}} = 0.57 \pm 0.01)$.

It is interesting also to note that when $\alpha \to 0$ the amplitude of the long-range component tends to zero while the short-range component in the low frequency limit becomes δ-function like. This result is also in a good qualitative agreement with the results of numerical simulations (see Fig. 7).

3.2 The non-local Boussinesq equation model

Here we also restrict ourselves to the case when the dispersive interaction is of the Kac-Baker type. In this case the quasicontinuum limit of the nonlocal Boussinesq equation (10) can be presented as follows [6]

$$(\partial_z^2 - \sigma_+^2)(\partial_z^2 - \sigma_-^2)w(z) = \frac{12}{v^2}(\partial_z^2 - \kappa^2)w^2(z)\,, \quad (35)$$

where the parameters $\sigma_\pm$ play the same role as the parameters $s_\pm$ in the previous subsection. They are given by

$$\sigma_\pm^2 = \frac{1}{2}\Bigg\{\kappa^2 + 12\frac{v^2-1}{v^2}$$
$$\pm\sqrt{\left(\kappa^2 - 12\frac{v^2-1}{v^2}\right)^2 + 48\kappa^2\frac{c^2-1}{v^2}}\Bigg\}\,, \quad (36)$$

where the speed of sound c in the lattice with the Kac-Baker interaction is determined by the expression

$$c = \left[1 + J\frac{\mathrm{e}^{-\alpha}+1}{(\mathrm{e}^{-\alpha}-1)^2}\right]^{1/2}\,. \quad (37)$$

The parameter σ_+ is finite at all velocities $v \geq c$ and tends to $\sqrt{12}$ for $v \to \infty$. The parameter σ_- vanishes at $v = c$ and tends to κ for $v \to \infty$. One can find that in the travel-wave approach the Hamiltonian is determined by the expressions

$$H = vP - M(v)\,, \quad (38)$$

where P is the canonical momentum and

$$M(v) = \frac{1}{6}\int_{-\infty}^{\infty} w^3(x)\mathrm{d}x \quad (39)$$

is the nonlinear part of the Hamiltonian.

Near the speed of sound excitations have a width much larger than σ_+^{-1} and can be described by equation (35) in the approximation $(\partial_z^2 - \sigma_+^2)w \approx -\sigma_+^2 w$. In this approximation the soliton solutions exist in a finite interval of velocities, $c < v < v_{\mathrm{cr}} \simeq \sqrt{(4c^2-1)/3}$. The explicit form of the low-velocity soliton in given in reference [6]. Using this expression it is straightforward to obtain the energy of the soliton belonging to the low-velocity branch in the form

$$H_< = vP_< - M_<(v)\,,$$
$$P_< = \frac{\sigma_+^4 v^5}{72\mathcal{A}^2\sigma_-}\left(\frac{\mathcal{A}-4}{3}I(w_1) + 2\right)\,,$$
$$M_<(v) = \frac{\sigma_+^6 v^6}{93312\,\mathcal{A}^3}\Bigg(\mathcal{A}^2 - 2\mathcal{A} + 40$$
$$- \frac{(\mathcal{A}-4)^2(\mathcal{A}+5)}{3}I(w_1)\Bigg)\,, \quad (40)$$

with

$$I(w) = \int_0^w \frac{1}{\mathcal{R}(x)}\mathrm{d}x$$
$$= \frac{1}{\sqrt{\mathcal{A}}}\ln\left(\left|\frac{\sqrt{\mathcal{A}\mathcal{R}(w)} + \mathcal{A}w - (\mathcal{A}+2)/3}{\sqrt{\mathcal{A}} - (\mathcal{A}+2)/3}\right|\right)\,,$$
$$\mathcal{R}(x) = \sqrt{\mathcal{A}x^2 - \frac{2}{3}(\mathcal{A}+2)x + 1}\,, \quad (41)$$

where $\mathcal{A} \equiv (\kappa^2/\sigma_-^2) > 4$ in the velocity interval $c < v < v_{\mathrm{cr}}$, and

$$w_1 = \frac{1}{3\mathcal{A}} \left(\mathcal{A} + 2 - \sqrt{(\mathcal{A}-1)(\mathcal{A}-4)} \right) \quad (42)$$

is the amplitude of the low-velocity soliton.

Far from the speed of sound we will use the same approach as in the previous subsection (see also Ref. [6]). We seek a solution of equation (10) as a sum

$$w(z) = w_{\mathrm{S}}(z) + w_{\mathrm{L}}(z) , \quad (43)$$

where $w_{\mathrm{S}}(z)$ is the short-range component of the strain and $w_{\mathrm{L}}(z)$ is the long-range one.

Assuming that the function $w_{\mathrm{S}}(z)$ satisfies the equation

$$\partial_z^2 w_{\mathrm{S}} - \left(\sigma_+^2 + \frac{24}{v^2} w_{\mathrm{L}}(0) \right) w_{\mathrm{S}} - \frac{12}{v^2} w_{\mathrm{S}}^2 = 0 , \quad (44)$$

we obtain from equation (35) an equation for $w_{\mathrm{L}}(z)$ in the form

$$\partial_z^2 \left(w_{\mathrm{L}} + \frac{12}{v^2 \sigma_+^2} w_{\mathrm{L}}^2 \right) - \sigma_-^2 w_{\mathrm{L}} - \frac{12\kappa^2}{v^2 \sigma_+^2} w_{\mathrm{L}}^2$$
$$= -\mathcal{B} \left(\kappa^2 - \sigma_-^2 \right) \delta(z) , \quad (45)$$

where

$$\mathcal{B} = \int_{-\infty}^{\infty} \mathrm{d}z\, w_{\mathrm{S}}(z) . \quad (46)$$

To obtain equations (44) and (45) we took into account the big difference in the short-range scale σ_+^{-1} and the long-range one σ_-^{-1} and proceeded in the same way as we did in the previous subsection. From equation (44) we get the short-range component w_{S} in the form

$$w_{\mathrm{S}}(z) = -\frac{1}{4} \sigma_+^2 v^2 (1 - 2\gamma) \operatorname{sech}^2 \left(\sqrt{1-2\gamma}\, \frac{\sigma_+ z}{2} \right) , \quad (47)$$

where $\gamma = 12\, |w_{\mathrm{L}}(0)| / (v\sigma_+)^2$ determines the amplitude of the long-range component. It can be found from the equation [6]

$$3(\mathcal{A} - 1) \frac{\sigma_-}{\sigma_+} = \frac{\gamma \mathcal{R}(\gamma)}{\sqrt{1-2\gamma}} . \quad (48)$$

Note that there is a misprint in the corresponding equation of reference [6]: one should omit $\bar{w}_{\mathrm{L}}(0)$ (which plays the same role as γ in this paper) in the denominator of the fraction in the l.h.s. of equation (A.19).

Using equations (47, 43), and (48) one can obtain that the energy of the compound soliton (43), *i.e.* the soliton which belongs to the high-velocity branch, can be presented in the form

$$H_> = vP_> - M_>(v) , \quad (49)$$

where

$$P_> = \frac{\sigma_+^4 v^5}{72} \left(\frac{3}{\sigma_+} \sqrt{1-2\gamma} \right.$$
$$\left. + \frac{1}{\mathcal{A}^2 \sigma_-} \left[2 + \frac{\mathcal{A}-4}{3} I(\gamma) - (2 + \mathcal{A}\gamma)\mathcal{R}(\gamma) \right] \right) \quad (50)$$
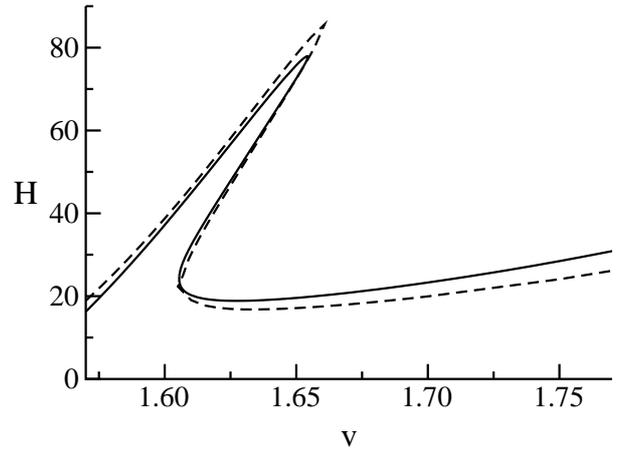

Fig. 8. Energy of the pulse solitons *versus* velocity in the anharmonic lattice with Kac-Baker ($s = 0$) long-range interaction calculated numerically (full line) and analytically (dashed line) for $\alpha = 0.05$ and $J = 0.0016$.

is the canonical momentum of the compound soliton and

$$M_>(v) = \frac{1}{2880} \sigma_+^5 v^6 \sqrt{1-2\gamma}\, (3\gamma^2 - 3\gamma + 2)$$
$$+ \frac{\sigma_+^6 v^6}{93320 \mathcal{A}^3} \left((\mathcal{A}^2 - 2\mathcal{A} + 40)(1 - \mathcal{R}(\gamma)) \right.$$
$$\left. - \mathcal{A}(\mathcal{A}+20)\gamma\mathcal{R}(\gamma) - \frac{(\mathcal{A}-4)^2(\mathcal{A}+5)}{3} I(\gamma) \right) \quad (51)$$

is the corresponding nonlinear part.

In the velocity interval $v > v_c$ ($\mathcal{A} < 4$) equation (48) for all values of the inverse radius α has a solution which tends to zero when $v \to \infty$. There is an one-to-one correspondence between the velocity of soliton and its energy. But when

$$\frac{\kappa^2(4c^2 - 1)}{c^2 - 1} \le \frac{64}{729} \quad (52)$$

Equation (48) has also two solutions in the interval $v < v_c$ ($\mathcal{A} > 4$). In other words under the condition (52), which taking into account the explicit form of the speed of sound (37), can be written as

$$J \ge \frac{3\alpha^4}{8(\alpha_0^2 - \alpha^2)} \quad (53)$$

with $\alpha_0 \approx 0.16$, there exist three stationary pulse solitons with different energy for each value of the velocity and the function $H(v)$ has a characteristic Z-shape (see Fig. 1). Comparing the dependence $H(v)$ obtained analytically from equations (40, 49–51) with the dependence obtained numerically shows a good agreement between the two approaches (see Fig. 8). The function (53) also describes very well the boundary which separates the area where $H(v)$ has a N-shape and a Z-shape (see Fig. 3 in Ref. [7]).

4 Conclusion

We investigated the effect of length scale competition in two systems which can bear pulse-like nonlinear excitations: a chain of coupled nonlinear oscillators (nonlinear Schrödinger model) and an anharmonic chain with cubic nearest-neighbor interaction. Two types of dispersive interactions were studied: the Kac-Baker interaction and screened Coulomb interaction. We have shown that the existence of two competing length scales: the radius of the dispersive interaction and lattice spacing provides the existence of two types of pulse solitons one of which is broad, continuum-like and uni-component, and another is narrow, discrete-like and has a compound structure. It consists of two components: short-ranged breather-like component which dominates near the center of the excitation and long-ranged component which contributes mainly to the tails of the excitation. These two stable solitons are separated by gap: an interval of spectral parameter (velocity in the case of Boussinesq equation and frequency in the case of nonlinear Schrödinger equation) where there are no stable stationary excitations. We show that the gap decreases when the radius of the dispersive interaction increases and it closes when the radius of the dispersive interaction exceeds some critical value. In contrast to systems with short-range and moderate-range dispersive interactions, where there is unambiguous correspondence between the velocity (frequency in the NLS equation) of the soliton and its energy, in systems where the length scales differ significantly (ultra-long-range interaction) there is an interval where three different states with different energies (momentum, number of quanta, etc.) correspond to each value of the spectral parameter. This is a generic property of all systems with competing length scales and is due to the compound structure of excitations.

References

1. S. Flach, C.R. Willis, Phys. Rep. **295**, 181 (1998).
2. E.W. Laedke, K.H. Spatschek, S.K. Turitsyn, Phys. Rev. Lett. **73**, 1055 (1994); E.W. Laedke, O. Kluth, K.H. Spatschek, Phys. Rev. E **54**, 4299 (1996).
3. B.A. Malomed, M.I. Weinstein, Phys. Lett. A **220**, 91 (1996).
4. S. Flach, K. Kladko, R.S. MacKay, Phys. Rev. Lett. **78**, 1207 (1997).
5. A. Neuper, Yu. Gaididei, N. Flytzanis, F.G. Mertens, Phys. Lett. A **190**, 165 (1994).
6. Yu. Gaididei, N. Flytzanis, A. Neuper, F.G. Mertens, Phys. Rev. Lett. **75**, 2240 (1995); Physica D **107**, 83 (1997).
7. S.F. Mingaleev, Yu.B. Gaididei, F.G. Mertens, Phys. Rev. E **58**, 3833 (1998).
8. Yu.B. Gaididei, S.F. Mingaleev, P.L. Christiansen, K.Ø. Rasmussen, Phys. Lett. A **222**, 152 (1996).
9. Yu.B. Gaididei, S.F. Mingaleev, P.L. Christiansen, K.Ø. Rasmussen, Phys. Rev. E **55**, 6141 (1997).
10. S.F. Mingaleev, Yu.S. Kivshar, R.A. Sammut, Phys. Rev. E **62**, 5777 (2000).
11. M. Johansson, Yu. B. Gaididei, P.L. Christiansen, K.Ø. Rasmussen, Phys. Rev. E **57**, 4739 (1998).
12. M. Johansson, S. Aubry, Yu.B. Gaididei, P.L. Christiansen, K.Ø. Rasmussen, Physica D **119**, 115 (1998).
13. Yu.B. Gaididei, P.L. Christiansen, K.Ø. Rasmussen, M. Johansson, Phys. Rev. B **55**, R13365 (1997).
14. M.V. Gvozdikova, A.S. Kovalev, Low Temp. Phys. **24**, 808 (1998) [Fiz. Nizk. Temp. **24**, 1077 (1998)].
15. S.F. Mingaleev, Yu.B. Gaididei, F.G. Mertens, Phys. Rev. E **61**, R1044 (2000).
16. W. Magnus, F. Oberhettinger, R.P. Soni, *Formulas and Theorems for the Special Functions of Mathematical Physics* (Springer-Verlag, Berlin-Heidelberg-New York, 1966).
17. P. Rosenau, Phys. Lett. A **118**, 222 (1986).